MODELLING BLOOD FLOW AND HEAT TRANSFER IN THE CARDIOVASCULAR SYSTEM OF HUMAN UNDERGOING TUMOR TREATMENT

***SALIHU, N. O., AIYESIMI, Y. M., JIYA, M., & ANDBOLARIN, G. A.**
Department of Mathematics,
Federal University of Technology, Minna, Nigeria
***Email:** so.nasiru@futminna.edu.ng **Phone No:** 08035789694

Abstract
This paperpresents a theoretical study of blood flow and heat transfer in the cardiovascular system of human undergoing tumor treatmentunder the action of an externally applied magnetic field. The fluid (blood) medium is assumed to be porous in nature. The variable viscosity of blood depending on hematocrit is taken into account in order to improve resemblance to the real situation. The temperature-dependent blood thermal conductivity is considered. The transient governing equations for laminar, incompressible Newtonian fluid and heat transfer is solved by using Olayiwola's Generalized Polynomial Approximation Method (OGPAM). The solutions are obtained for flow velocity and heat transfer in both tissue and blood. The computations were done using Computer Symbolic Algebraic Package MAPLE 17 version and the results are presented graphically. It is observed that the influence of hematocrit, magnetic field, permeabilty parameter, Reynolds number and Pressure gradient have important impact on the velocity profile. Moreover, the effect of Peclet number, pressure gradient and perfusion mass flow rate on the tissue and blood temperature profiles has been significantly observed. It can be concluded from the results obtained that the flow of blood can be controlled by the application of an external magnetic field.

Keywords: Blood flow, Cardiovascular system, heat transfer, Hematocrit, thermal conductivity

Introduction

The cardiovascular system is the blood transport mechanism that enables the nutrient transport to the tissues and organs of the body and the removal of various waste and toxic substances (Urquiza *et al*., 2005). It consists of three major components listed as the heart (the system's pump that pump blood around the body), the blood vessel (the delivery routes like) and the blood (a fluid that contains the needed oxygen and nutrients for the body and carries the wastes that needed to be removed). Generally, the cardiovascular system comprises of two connected distinct systems: The systemic circulation that provide organs, tissues and cells with blood so that they can get oxygen and other vital substances (Taura *et al*., 2012), the pulmonary circulation where the fresh oxygen we breathe in flows into the blood. Simultaneously, carbon dioxide is being released from the blood.The major function of cardiovascular system is to support blood flow to all parts of the body for its survival.

The examination of heat transfers and blood flow in biological processes demands exact or careful mathematical models. The biological processes normally involve two stages namely solid and liquid (fluid). Thermal ablation therapy is an application of heat transfer and fluid flow in biological processes. Temperature plays an important role with tissue interactions (Aiyesimi & Salihu, 2016). The blood flow in a tissue mainly has a direction from artery to vein passing through the capillary bed, the blood and its surrounding tissues are not in thermal equilibrium when the blood vessel diameter is larger which means the energy equations for tissue and blood in large vessels must be treated one at a time. One of the crucial issues of thermal treatments is blood flow. Blood flow usually drains the free heat from the heating region, which causes inadequate thermal dose in the targeted volume.

The studies of blood flow via a porous medium have gained serious attention to the medical practitioners as a result of its massive changes in the flow conditions. Dash *et al*. (1996) studied the Brinkman equation to model the flow of blood when there is an accumulation of fatty plaques in the lumen of an arterial part. They treated the clogged segment as a porous medium. Bhargava *et al*. (2007) analyzed the transport of pharmaceutical species in laminar, homogeneous, incompressible, magneto-hydrodynamic, pulsating flow via two dimensional channels with a porous wall containing non-porous materials. Misra and Shit (2007) and Misra *et al.* (2011) considered a mathematical model and numerical model for analyzing blood flow via a porous vessel with a magnetic field where the viscosity varies in the radial direction. Shit and Roy (2012) presented a paper on a theoretical study of blood flow through a tampered and overlapping stenosed artery under the action of an externally applied magnetic field with the blood medium assumed to be porous in nature. The variable viscosity of blood depending on hematocrite (percentage volume of erythrocytes) is taken into account.

The mathematical equations governingblood flow and heat transfer in the cardiovascular system of a human undergoing hyperthermia treatment is presented and solved using Olayiwola's Generalized Polynomial Approximation Method (OGPAM). The graphical summaries of the system responses is also considered.

Problem Formulation

Here, the blood is assumed to be incompressible and has uniform dense throughout but the viscosity $\mu(r)$ varies in the radial direction. The work of Shit and Roy (2017) is extended with the equation governing the blood flow under a closed watch of an external magnetic field via blood as follow:

$$\rho\frac{\partial w}{\partial t}=-\frac{\partial p}{\partial z}+\frac{1}{r}\frac{\partial}{\partial r}\left(r\mu(r)\frac{\partial w}{\partial r}\right)-\sigma B_0^2 w-\frac{\mu(r)}{\bar{k}}w \tag{1}$$

Einsten's formula for the variable viscosity of blood is taken to be

$$\mu(r)=\mu_0\left(1+\beta h(r)\right) \tag{2}$$

The analysis will be carried out by using the following empirical formula for hematocrit given by

$$h(r)=H\left(1-\left(\frac{r}{R_0}\right)^m\right) \tag{3}$$

The work of Horng *et al*. (2015) is also extended with the governing equations of the temperature evolution for the tissue andblood vessels as follow:

$$\rho_t c_t\frac{\partial T_t}{\partial t}=k_t\frac{1}{r}\frac{\partial}{\partial r}\left(r\frac{\partial T_t}{\partial r}\right)+k_t\frac{\partial}{\partial z}\left(\frac{\partial T_t}{\partial z}\right)-W_b c_b\left(T_t-T_a\right)+Q_t\left(r,z,t\right) \tag{4}$$

$$\rho_b c_b\left(\frac{\partial T_b}{\partial t}+w\frac{\partial T_b}{\partial z}\right)=\left(\frac{1}{r}\frac{\partial}{\partial r}\left(k_b r\frac{\partial T_b}{\partial r}\right)+\frac{\partial}{\partial z}\left(k_b\frac{\partial T_b}{\partial z}\right)\right)+Q_b\left(r,z,t\right) \tag{5}$$

We adopt no-slip boundary condition at the vessel wall and we put into consideration the axis-symmetric boundary condition of axial velocity at the mid line of the vessel with the assumptions that the blood vessel segment is straight, that the vessel wall is rigid and porous. Also, we assume that the flow is laminar, incompressible and Newtonian. Thus, the initial and boundary conditions are formulated as:

$$\left.\begin{array}{llllll} w(r,z,0)=0, & \left.\dfrac{\partial w}{\partial r}\right|_{r=0}=0, & \left.\dfrac{\partial w}{\partial z}\right|_{r=0}=0, & w(R_0,z,t)=0, & w(r,L,t)=0 \\ T_t(r,z,0)=T_a, & \left.\dfrac{\partial T_t}{\partial r}\right|_{r=0}=0, & \left.\dfrac{\partial T_t}{\partial z}\right|_{r=0}=0, & T_t(R_0,z,t)=T_a, & T_t(r,L,t)=T_a \\ T_b(r,z,0)=T_a, & \left.\dfrac{\partial T_b}{\partial r}\right|_{r=0}=0, & \left.\dfrac{\partial T_b}{\partial z}\right|_{r=0}=0, & T_b(R_0,z,t)=T_a, & T_b(r,L,t)=T_a \end{array}\right\} \quad (6)$$

Where z is the axial distance, r is the radial distance, ρ is the density, w is the axial velocity of blood flow, w_0 is the initial axial velocity of blood flow, p is the blood pressure, $\mu(r)$ is the blood viscosity at a radial distance r, $h(r)$ is the hematocrit at a distance r, H is the maximum hematocrit at the center of the artery, μ_0 is the coefficient of viscosity of plasma, R_0 is the radius of a normal arterial segment, β is a constant whose value for blood is equal to 2.5, σ is the electrical conductivity, B_0 is the applied magnetic field strength, k is the permeability of the porous medium, k_t is the thermal conductivity of tissue, k_b is the thermal conductivity of blood, c_t is the specific heat capacity of tissue, c_b is the specific heat capacity of blood, T_t is the tissue temperature, T_b is the blood temperature, T_a is the ambient temperature that is normally assumed to be 37^0C, W_b is the perfusion mass flow rate, $Q_t(r,z,t)$ is the tissue power of heat added axis symmetrically, $Q_b(r,z,t)$ is the blood power of heat added axis symmetrically and L is the length of vessel wall.

Dimensional Analysis

We non–dimensionalize equations (3.1) – (3.8) using the following dimensionless variables:

$$\left.\begin{array}{lllll} r'=\dfrac{r}{R_0}, & \tau=\dfrac{w_0 t}{R_0}, & z'=\dfrac{z}{L}, & \phi=\dfrac{w}{w_0}, & \alpha=\dfrac{T_b}{T_t} \\ \theta=\dfrac{T_t-T_a}{\alpha T_a}, & \psi=\dfrac{T_b-T_a}{\alpha T_a}, & p'=\dfrac{p}{\rho w_0^2} & & \end{array}\right\} \quad (7)$$

Therefore, the dimensionless equations with their initial and boundary conditions are:

$$\frac{\partial\phi}{\partial\tau}=D+\frac{1}{\mathrm{Re}}\frac{1}{r}\frac{\partial}{\partial r}\left(r\left(1+\beta H\left(1-r^m\right)\right)\frac{\partial\phi}{\partial r}\right)-\frac{M^2}{\mathrm{Re}}\phi-\frac{k_p}{\mathrm{Re}}\left(1+\beta H\left(1-r^m\right)\right)\phi \quad (8)$$

$$\frac{\partial\theta}{\partial\tau}=+\frac{1}{Pe_1}\frac{1}{r}\frac{\partial}{\partial r}\left(r\left(1+\alpha\theta\right)\frac{\partial\theta}{\partial r}\right)+\frac{1}{Pe_2}\frac{\partial}{\partial z}\left(\frac{\partial\theta}{\partial z}\right)-\alpha_1\theta+\gamma_1\frac{\pi}{2}\sin\left(\frac{\pi_t}{t_h}\right) \quad (9)$$

$$\frac{\partial\psi}{\partial\tau}+a\phi\frac{\partial\psi}{\partial z}=\frac{1}{Pe_3}\frac{1}{r}\frac{\partial}{\partial r}\left(r\left(1+\alpha\theta\right)\frac{\partial\psi}{\partial r}\right)+\frac{1}{Pe_4}\frac{\partial}{\partial z}\left(\left(1+\alpha\theta\right)\frac{\partial\theta}{\partial z}\right)+\gamma_2\frac{\pi}{2}\sin\left(\frac{\pi_t}{t_h}\right) \quad (10)$$

$$\left.\begin{array}{l}\phi(r,\,z,\,0)=0,\ \left.\dfrac{\partial\phi}{\partial r}\right|_{r=0}=0,\ \left.\dfrac{\partial\phi}{\partial z}\right|_{z=0}=0,\ \ \phi(1,\,z,\,t)=0,\ \phi(r,\,1,\,t)=0\\ \theta(r,\,z,\,0)=0,\ \left.\dfrac{\partial\theta}{\partial r}\right|_{r=0}=0,\ \left.\dfrac{\partial\theta}{\partial z}\right|_{z=0}=0,\ \ \theta(1,\,z,\,t)=0,\ \theta(r,\,1,\,t)=0\\ \psi(r,\,z,\,0)=0,\ \left.\dfrac{\partial\psi}{\partial r}\right|_{r=0}=0,\ \left.\dfrac{\partial\psi}{\partial z}\right|_{z=0}=0,\ \ \psi(1,\,z,\,t)=0,\ \psi(r,\,1,\,t)=0\end{array}\right\} \tag{11}$$

Transformation

We introduced a new space variable as:

$$2\eta = r + z \tag{12}$$

Then, equations (8) – (11) reduced to

$$\frac{\partial\phi}{\partial\tau}=-D+\frac{1}{4\,\mathrm{Re}}\frac{1}{\varepsilon}\frac{\partial}{\partial\eta}\left(\varepsilon\left(1+\beta H\left(1-\varepsilon^{m}\right)\right)\frac{\partial\phi}{\partial\eta}\right)-\frac{M^{2}}{\mathrm{Re}}\phi-\frac{k_{p}}{\mathrm{Re}}\left(1+\beta H\left(1-\varepsilon^{m}\right)\right)\phi \tag{13}$$

$$\frac{\partial\theta}{\partial\tau}=\frac{1}{4Pe_{1}}\frac{1}{\varepsilon}\frac{\partial}{\partial\eta}\left(\varepsilon\frac{\partial\theta}{\partial\eta}\right)+\frac{1}{4Pe_{2}}\frac{\partial}{\partial\eta}\left(\frac{\partial\theta}{\partial\eta}\right)-\alpha_{1}\theta+\gamma_{1}\frac{\pi}{2}\sin\left(\frac{\pi_{t}}{t_{h}}\right) \tag{14}$$

$$\frac{\partial\psi}{\partial\tau}+\frac{a}{2}\phi\frac{\partial\psi}{\partial\eta}=\frac{1}{4Pe_{3}}\frac{1}{\varepsilon}\frac{\partial}{\partial\eta}\left(\varepsilon\left(1+\alpha\theta\right)\frac{\partial\psi}{\partial\eta}\right)+\frac{1}{4Pe_{4}}\frac{\partial}{\partial\eta}\left(\left(1+\alpha\theta\right)\frac{\partial\psi}{\partial\eta}\right)+\gamma_{2}\frac{\pi}{2}\sin\left(\frac{\pi_{t}}{t_{h}}\right) \tag{15}$$

$$\left.\begin{array}{l}\phi(\eta,\,0)=0,\ \left.\dfrac{\partial\phi}{\partial\eta}\right|_{\eta=0}=0,\ \ \phi(1,\,\tau)=0\\ \theta(\eta,\,0)=0,\ \left.\dfrac{\partial\theta}{\partial\eta}\right|_{\eta=0}=0,\ \ \theta(1,\,\tau)=0\\ \psi(\eta,\,0)=0,\ \left.\dfrac{\partial\psi}{\partial\eta}\right|_{\eta=0}=0,\ \ \psi(1,\,\tau)=0\end{array}\right\} \tag{16}$$

Method of Solution

In other to solve equations (13) – (16), the Olayiwola's generalized polynomial approximation method(OGPAM) (Olayiwola, 2022) is employed and we obtain

$$\phi(\eta,t)=\frac{B_{2}}{B_{1}}\left(1-e^{B_{1}t}\right)\left(1-\eta^{2}\right) \tag{17}$$

$$\theta(\eta,t)=\frac{B_{6}}{B_{5}}\left(1-e^{-B_{5}t}\right)\left(1-\eta^{2}\right) \tag{18}$$

$$\psi(\eta,t)=\left.\psi\right|_{\eta=0}\left(1-\eta^{2}\right) \tag{19}$$

Where,

$$B_0 = \begin{pmatrix} \left(\frac{(2-z)^{m+1}}{2(m+1)} - \frac{z^{m+1}}{2(m+1)}\right)\left(\frac{2}{4\mathrm{Re}} + \frac{k_p}{\mathrm{Re}}\right)\beta H - \\ \frac{4(1+\beta H)}{4\mathrm{Re}}\left(\frac{1}{2} + \frac{\ln\left(\frac{z-2}{z}\right)z}{4}\right) - \\ \frac{2M^2}{3\mathrm{Re}} - \frac{2}{3}\frac{k_p}{\mathrm{Re}}(1+\beta H) + \frac{4\beta H}{4\mathrm{Re}}(m+1)\left(\frac{2^{m-1}}{m+1} - \frac{(m-1)2^{m-2}z}{m} + \right) - \\ (m-2)2^{m-2}z^2 \\ \frac{k_p}{\mathrm{Re}}\beta H\left(\frac{2^m}{m+3} - \frac{2^{m-1}mz}{m+2} + \frac{2^{m-3}m(m-1)z^2}{(m+1)}\right) \end{pmatrix} \quad (20)$$

$$B_1 = \frac{3}{2}(B_0) \quad (21)$$

$$B_2 = \frac{3D}{2} \quad (22)$$

$$B_3 = 2\left(\frac{1}{4Pe_1}\left(\frac{1}{2} + \frac{\ln\left(\frac{z-2}{z}\right)z}{4}\right) - \frac{\alpha_1}{3}\right) \quad (23)$$

$$B_4 = \gamma_1 \frac{\pi}{2}\sin\left(\frac{\pi_t}{t_h}\right) \quad (24)$$

$$B_5 = \frac{3}{2}\left(\frac{p}{2}(-2+2) + B_3\right) \quad (25)$$

$$B_6 = \frac{3}{2}B_4 \quad (26)$$

$$B_7 = \begin{pmatrix} -\frac{2\alpha B_6}{4Pe_3}\left(\frac{1}{16}ln(-z)z^3 - \frac{1}{4}zln(-z) + \frac{1}{3} - \frac{1}{8}z - \frac{1}{8}z^3 - \right) + \frac{aB_2}{4} \\ \frac{1}{16}ln(2-z)z^3 + \frac{1}{4}z\ln(2-z) \end{pmatrix} \quad (27)$$

$$B_8 = \left(\frac{1}{2} + \frac{\ln\left(\frac{z-2}{z}\right)z}{4}\right) \quad (28)$$

$$B_9 = \gamma_2 \frac{\pi}{2} \sin\left(\frac{\pi_t}{t_h}\right) \tag{29}$$

$$B_{10} = \left(-\frac{q}{2}(-2+2) + B_8\right) \tag{30}$$

$$B_{11} = \frac{3}{2} B_9 \tag{31}$$

$$\psi\Big|_{\eta=0} = e^{-\frac{3}{2}\left(B_{10}t - \frac{1}{2}B_7 t^2\right)} \left(\sqrt{\frac{\pi}{3B_7}} B_{11} e^{\frac{3}{4}\frac{B_{10}^2}{B_7}} \left(erf\left(\frac{B_{10}}{2}\sqrt{\frac{3}{B_7}}\right) + erf\left(\frac{\sqrt{3}\left(B_7 t - B_{10}\right)}{2\sqrt{B_7}}\right)\right)\right) \tag{32}$$

Results and Discussions

In this analysis, we solved the equations governing the blood flow and heat transfer in the cardiovascular system of human undergoing tumor treatment analytically using OGPAM. This is to see the effect of parameters involved on the axial velocity of blood flow, tissue temperature and blood temperature. Finally, we examined the effect of the Permeability parameter (k), Peclet number (P_{e1}), Pressure gradient parameter (C), Perfusion mass flow rate (α_1), Temperatures ratio (α), Hartman number (M) on the velocity and temperatures. The computations were done using computer symbolic algebraic package MAPLE 17.

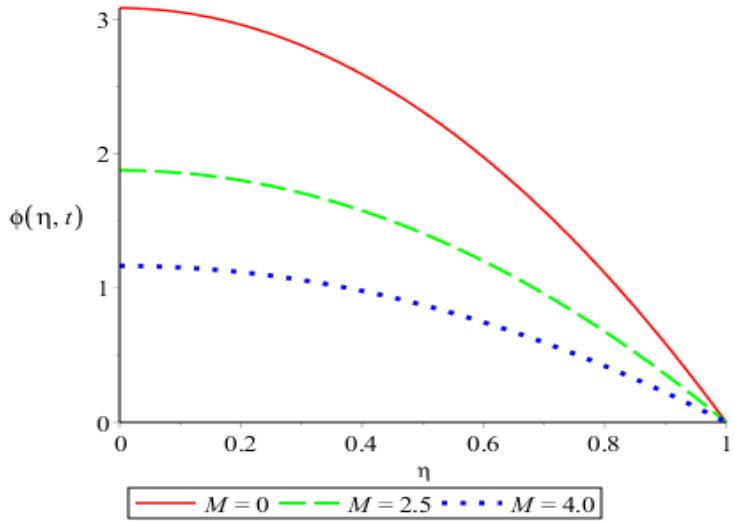

Figure 1: Graph of velocity against distance for different values of Hartmann number

Figure 1 displays the graph of velocity profile $\phi(\eta,t)$ for different values of Hartmann number (M). It is observed that velocity decreases along the distance and this velocity decreases as Hartmann number increases.

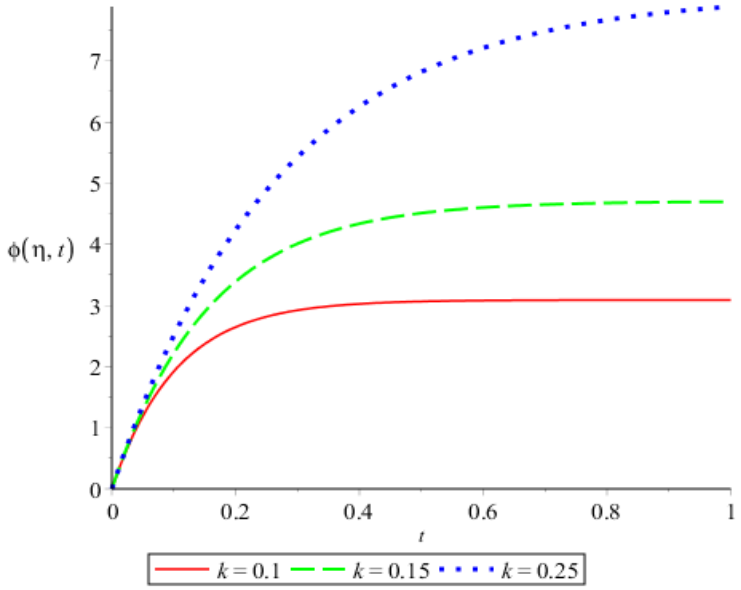

Figure 2: Graph of velocity against time for different values of permeability Parameter

Figure 2 shows the graph of velocity profile $\phi(\eta,t)$ for different values of permeability parameter (k). It is observed that velocity increase and later became steady with time and maximum velocity increases as value permeability parameter increases.

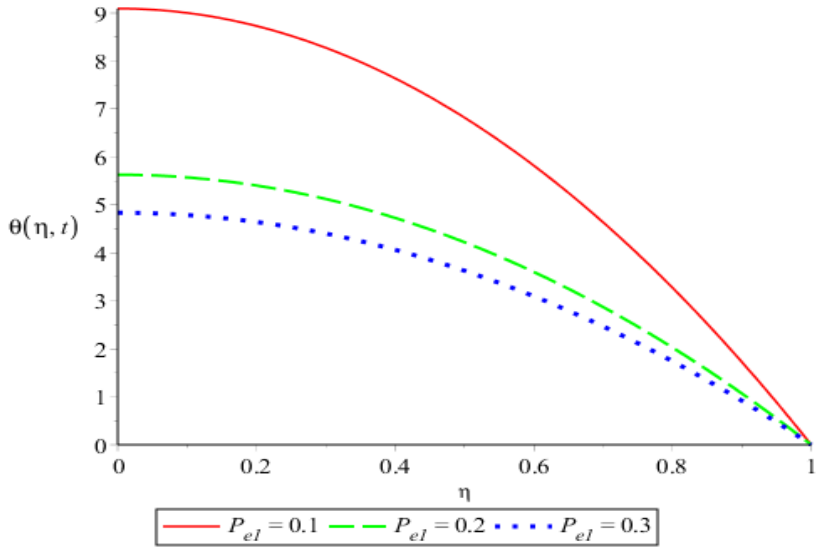

Figure 3: Graph of tissue temperature against distance for different values of Peclet number

Figure 3 shows the graph of tissue temperature profile $\theta(\eta,t)$ for different values of Peclet number (P_{e1}). It is observed that tissue temperature decreases along the distance and this temperature increases as Peclet number increases.

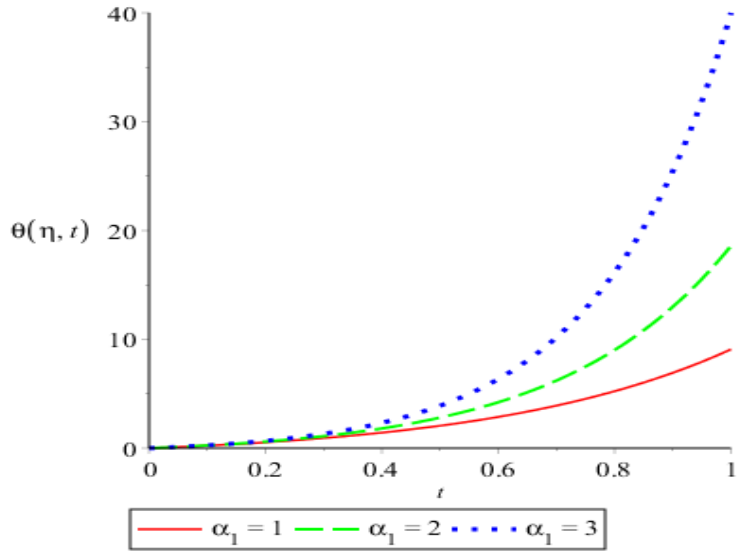

Figure 4: Graph of tissue temperature against time for different values of perfusion mass flow rate

Figure 4 depicts the graph of tissue temperature profile $\theta(\eta,t)$ for different perfusion mass flow rate (α_1). It is observed that tissue temperature increase with time and maximum temperature increases as perfusion mass flow rate increases.

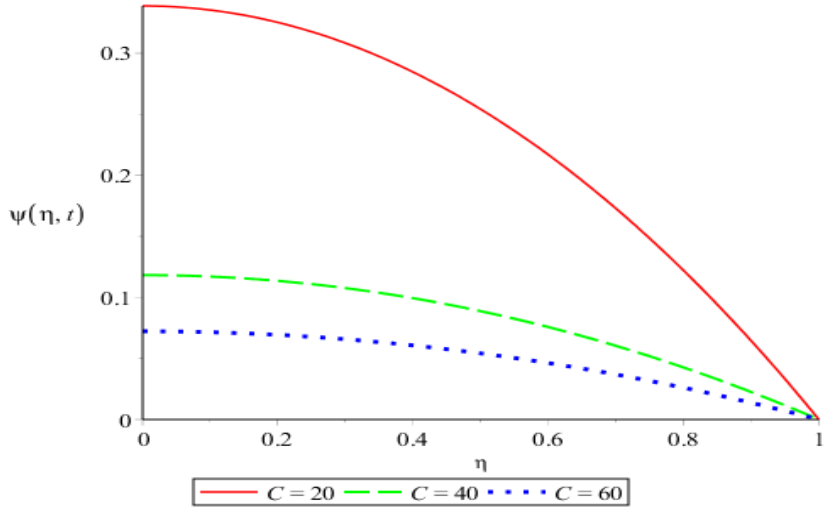

Figure 5: Graph of blood temperature against distance for different values of pressure gradient parameter

Figure 5 shows the graph of blood temperature profile $\psi(\eta,t)$ for different values of pressure gradient parameter (C). It is observed that blood temperature decreases along the distance and this temperature decreases as values of pressure gradient increases.

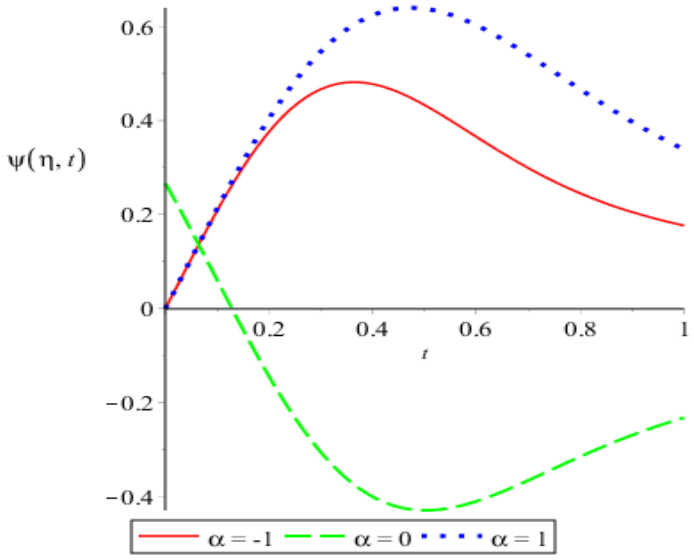

Figure 6: Graph of blood temperature against time for different values of temperatures ratio

Figure 6 depicts the graph of blood temperature profile $\psi(\eta,t)$ against time for different values of temperature ratio (α). It is observed that we have positive blood temperature profile when $\alpha<0$ and $\alpha>0$ while we have negative blood temperature profile when $\alpha=0$. This by implication means that variable thermal conductivity bring about increase in blood temperature.

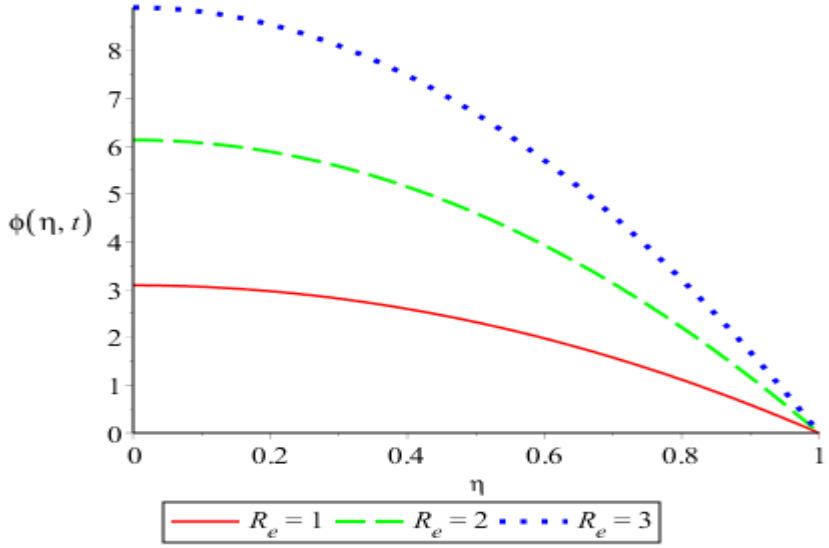

Figure 7: Graph of velocity against distance for different values of Reynolds number

Figure 7 displays the graph of velocity profile $\phi(\eta,t)$ for different values of Reynolds number (R_e). It is observed that velocity decreases along the distance and this velocity increases as Reynolds number increases.

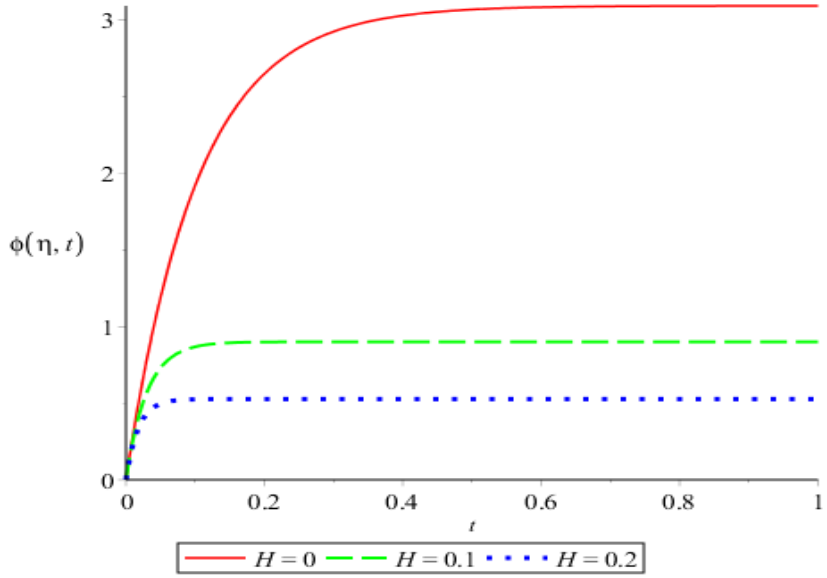

Figure 8: Graph of velocity against time for different values of hematocrit

Figure 8 shows the graph of velocity profile $\phi(\eta,t)$ for different values of hematocrit (H). It is observed that velocity increase and later became steady with time and maximum velocity decreases as values of hematocrit increases.

Conclusion

For variable viscosity and blood thermal conductivity, we have solved the equations governing the blood flow and heat transfer in the cardiovascular system of human undergoing tumor treatment analytically using OGPAM. The effects of the dimensionless parameters as shown on the graphs were analyzed. From the results obtained, all the parameters have appreciable impact on the system.

References

Aiyesimi Y. M., & Salihu O. N.(2016). Effects of Pollutants and Atmospheri Temperature Rise on Agriculture. *Journal of the Nigerian Association of Mathematical Physics,* 35, 115 – 124.

Bhargava, R., Rawat, S., Takhar, H. S., & Beg, O. A. (2007). Pulsatile magneto-biofluid flow and mass transfer in a non-Darcian porous medium channels. *Meccanica,* 42(4), 247–262.

Dash, R. K., Mehta, K. N., & Jayaraman, G. (1996). Casson fluid flowin a pipe filled with homogeneous porous medium, *International Journal of Engineering Science* 34(6), 1146–1156.

Horng, T. L., Lin, W. L., Liauh, C. T., & Shih, T. C. (2015). Effects of pulsatile blood flow in large vessels on thermal dose distribution during thermal therapy. *American Association of Physicists in Medicine*, 34, 1312–1320.

Misra, J. C., & Shit, G. C. (2007). Role of slip velocity in blood flow through stenosed arteries: A non-Newtonian model, *Journal of Mechanics in Medicine and Biology* 7(2007), 337–353.

Misra, J. C., Sinha, A., & Shit, G. C. (2011). Mathematical modeling of blood flow in a porous vessel having double stenoses in the presence of an external magnetic field, *International Journalof Biomathematics,* 4(2), 207–225.

Olayiwola, R. O. (2022): *Solving parabolic equations by Olayiwola's generalized polynomial approximation method*, International Journal of Mathematical Analysis and Modelling, 5(3): 24 – 43, October.

Shit, G. C., & Roy, M. (2012). Hydromagnetic pulsating flow of blood in a constricted porous channel: A theoretical study, in: *Proceedingsof the world congress on Engineering*, London, UK, 1. 83–88.

Shit, G. C., & Roy, M. (2017). Pulsatile flow and heat transfer of a magneto micropolar fluid through a stenosed artery under the influence of body acceleration, *Journal of Mechanics in Medicine and Biology,* 11 (5), 643–661.

Taura, L. S., Ishiyaku, I. B., & Kawo, A. H. (2012). The use of continuity equation of fluid mechanics to reduce the abnormality of the cardiovascular system: A control mechanics of the human heart. *Journal of Biophysics and Structural Biology,* 4(1), 1-12.

Urquiza, S. A., Blanco, P. J., Venere, M. J., & Feijoo, R. A. (2005). Multidimensional Modeling for the Carotid Artery Blood Flow. *Elsevier Science Direct*, 45, 131 – 149.